

Intracranial vessel wall lesions on 7T MRI and MRI features of cerebral small vessel disease: The SMART-MR study

Journal of Cerebral Blood Flow & Metabolism
2021, Vol. 41(6) 1219–1228
© The Author(s) 2020



Article reuse guidelines:
sagepub.com/journals-permissions
DOI: 10.1177/0271678X20958517
journals.sagepub.com/home/jcbfm



Maarten HT Zwartbol¹ , Anja G van der Kolk¹, Hugo J Kuijf² , Theo D Witkamp¹, Rashid Ghaznawi^{1,3} , Jeroen Hendrikse¹ and Mirjam I Geerlings³; on behalf of the UCC-SMART Study Group*

Abstract

The etiology of cerebral small vessel disease (CSVD) is the subject of ongoing research. Although intracranial atherosclerosis (ICAS) has been proposed as a possible cause, studies on their relationship remain sparse. We used 7 T vessel wall magnetic resonance imaging (MRI) to study the association between intracranial vessel wall lesions—a neuroimaging marker of ICAS—and MRI features of CSVD. Within the SMART-MR study, cross-sectional analyses were performed in 130 patients (68 ± 9 years; 88% male). ICAS burden—defined as the number of vessel wall lesions—was determined on 7 T vessel wall MRI. CSVD features were determined on 1.5 T and 7 T MRI. Associations between ICAS burden and CSVD features were estimated with linear or modified Poisson regression, adjusted for age, sex, vascular risk factors, and medication use. In 125 patients, ≥ 1 vessel wall lesions were found (mean 8.5 ± 5.7 lesions). ICAS burden (per + 1 SD) was associated with presence of large subcortical and/or cortical infarcts (RR = 1.65; 95%CI: 1.12–2.43), lacunes (RR = 1.45; 95% CI: 1.14–1.86), cortical microinfarcts (RR = 1.48; 95%CI: 1.13–1.94), and total white matter hyperintensity volume ($b = 0.24$; 95%CI: 0.02–0.46). Concluding, patients with a higher ICAS burden had more CSVD features, although no evidence of co-location was observed. Further longitudinal studies are required to determine if ICAS precedes development of CSVD.

Keywords

Intracranial atherosclerosis, cerebral small vessel disease, white matter hyperintensities, lacunes of presumed vascular origin, vessel wall imaging

Received 30 December 2019; Revised 11 August 2020; Accepted 16 August 2020

Introduction

Cerebral small vessel disease (CSVD), a common finding in the ageing brain, is used to describe a group of pathological changes affecting the small arteries, arterioles, capillaries, and venules of the brain.¹ It is thought to be one of the major causes of ischemic stroke.¹ Furthermore, it is one of the leading causes of vascular dementia and is a key contributor to the incidence of Alzheimer's disease.¹ Magnetic resonance imaging (MRI) features of CSVD include: recent small subcortical infarcts, white matter hyperintensities, microbleeds, lacunes of presumed vascular origin, prominent perivascular spaces, and brain atrophy.²

Although the MRI features are generally considered to be caused by ischemia, the etiological mechanisms

¹Department of Radiology, University Medical Center Utrecht and Utrecht University, Utrecht, the Netherlands

²Image Sciences Institute, University Medical Center Utrecht, Utrecht, the Netherlands

³Julius Center for Health Sciences and Primary Care, University Medical Center Utrecht and Utrecht University, Utrecht, the Netherlands

*Listed in Acknowledgements

Corresponding author:

Mirjam I Geerlings, Department of Epidemiology, Julius Center for Health Sciences and Primary Care, University Medical Center Utrecht, P.O. Box 85500, Stratenum 6.131, 3508 GA Utrecht, The Netherlands.
Email: m.geerlings@umcutrecht.nl

leading up to this stage remain to be elucidated.³ A wide range of potential mechanisms has been proposed, going from intrinsic disease of the smaller vessels (e.g. lipohyalinosis) to more extrinsic causes, e.g. emboli, atheroma of parent artery, or perforating arteriole, impaired cerebral blood flow, to non-ischemic causes, e.g. capillary endothelial failure.^{3,4}

The current view is that intrinsic changes of the small vessels are likely the dominant etiology.⁴ Intracranial atherosclerosis (ICAS)—which can cause atheroma, emboli, and impaired cerebral blood flow—has largely been dismissed as a major CSVD etiology.^{4–6} However, in the well-known (clinico)pathological study on lacunes by Fisher, ICAS and emboli accounted for the majority of lacunes.⁷ Several studies in Asian populations have observed this association in vivo as well.^{8,9} In our view, this warrants further study, because a better understanding of the cause of MRI features of CSVD might help explain the heterogeneous results regarding risk factors and clinical symptoms.¹⁰

A limitation of prior neuroimaging studies into ICAS is that most are based on angiography or transcranial Doppler, which can only assess luminal stenosis in the larger proximal cerebral arteries. Hence, plaques without stenosis, e.g. because of arterial remodeling, cannot be assessed. This is of importance because most CSVD lesions are chronic, which means that arterial remodeling—leading to a normalization of the arterial lumen—could have taken place in the meantime, hindering the ability to find a potential association between ICAS and CSVD lesions.¹¹ Furthermore, non-stenotic plaques can still cause emboli or stenosis of the ostia of subcortical perforators.

Vessel wall MRI can be used to image the actual vessel wall, making it possible to detect arterial vessel wall thickening independently from stenosis, leading to a significant improvement in plaque detection,^{12,13} with 7T MRI adding further improvement.^{14,15} Of note, intracranial vessel wall lesions have been associated with vascular risk factors¹⁶ and markers of extracranial atherosclerosis,¹⁷ supporting its use as a neuroimaging marker of ICAS burden.

In the current study, we set out to determine the association between the number of vessel wall lesions and MRI features of CSVD in a population of older adults with a history of vascular disease.

Materials and methods

Study sample

The Second Manifestations of ARterial disease—Magnetic Resonance (SMART-MR) study, an ongoing prospective cohort study at our institution, focuses on

neuroimaging MRI markers in patient with symptomatic atherosclerotic disease.¹⁸ From May 2001 to December 2005, patients newly referred to our institution with coronary artery disease, cerebrovascular disease, peripheral artery disease, or an abdominal aortic aneurysm, and without contraindications for MRI, were included. On a one-day visit, patients underwent extensive examinations, including a 1.5T brain MRI, physical examination, ultrasonography of the carotid arteries, blood and urine sampling, and questionnaires to assess risk factors, medical history, and daily functioning.¹⁹ Follow-up of 1.5T brain MRI, cognitive functioning, and depression assessment were performed from 2006 to 2009,²⁰ and from 2013 to 2017.¹⁶ During the most recent follow-up, a 7T brain MRI was included in the standard research protocol. Within this period, from June 2016 to October 2017, a vessel wall MRI sequence was added to the 7T brain MRI protocol.

In this study, we included all patients who had 7T vessel wall MRI performed during this period, which led to a total of 147 patients.¹⁶ We excluded 17 patients from the final analysis, leaving 130 patients, because of artifacts inhibiting vessel wall assessment of ≥ 1 major segment of the Circle of Willis (major segments included the distal internal carotid artery and primary branches (M1, A1, P1) of the anterior, middle, and posterior cerebral artery). Excluded patients did not differ in sex (88% vs. 88% male; $p=0.95$, χ^2 -test) and were not significantly older (70 ± 7 vs. 68 ± 9 years; $p=0.11$, Student's t-test). Vascular risk factor assessment, including questionnaire data and blood and urine sampling, was available from median (range) 2.3 (0.6–8.6) years prior to the 7T brain MRI.

The SMART-MR study was approved by the medical ethics committee of the University Medical Center Utrecht according to the guidelines of the Declaration of Helsinki of 1975 and written informed consent was obtained from all participants.

Covariates

Questionnaires were used to assess age, sex, educational level, alcohol use, smoking habits, and medication use. Weight and height measurements were taken for calculation of the body mass index (BMI; kg/m^2). Educational level was classified into seven categories, ranging from primary school to academic degree, according to the Dutch educational system. Systolic blood pressure (SBP; mmHg) and diastolic blood pressure (DBP; mmHg) were measured with a sphygmomanometer and defined as the average of three separate measurements. Venous blood samples were taken after an overnight fast. Diabetes was defined as a fasting serum glucose level of >11.1 mmol/L, a history of

diabetes, or use of antidiabetic medication at baseline or follow-up. Cholesterol levels were determined. An experienced technician performed carotid ultrasonography with a 10 MHz linear-array transducer. Carotid stenosis was defined according to standard criteria based on the peak systolic velocity.²¹ Mean carotid intima-media thickness was calculated from six measurements (anterolateral, posterolateral, and mediolateral in both common carotid arteries). Ankle-brachial index measurement was performed by experienced technicians, and was calculated from the highest SBP measured in both brachial arteries (using a semiautomatic oscillometric device in supine position), and the posterior tibial and dorsal pedal arteries (using Doppler ultrasound).

1.5T MRI protocol

A 1.5T whole-body system (Gyrosan ACS-NT, Philips Medical Systems, Best, the Netherlands) was used performing a standard protocol: a T1-weighted sequence (3D acquisition; repetition time (TR)/echo time (TE): 7.0/3.2 ms; voxel size = $0.94 \times 0.94 \times 1.0 \text{ mm}^3$ isotropic), a T1-weighted inversion recovery sequence (2D acquisition; TR/TE: 2900/22 ms; TI = 410 ms), a T2-weighted sequence (2D acquisition; TR/TE: 2200/10.5 ms), and a fluid-attenuated inversion recovery (FLAIR) sequence (2D acquisition; TI/TR/TE: 2000/6000/100 ms). All two-dimensional sequences were acquired with a voxel size of $1.0 \times 1.0 \times 4.0 \text{ mm}^3$ and contiguous slices. A phase-contrast MR angiography sequence (2D slice acquisition; TR/TE: 16/9 ms; voxel size = $0.98 \times 0.98 \times 5.00 \text{ mm}^3$; velocity sensitivity 100 cm/s; acquisition at the level of the proximal cavernous segment of the ICA and prepontine basilar artery) was also performed.

7T MRI protocol

A 7.0T whole-body MRI system (Philips Healthcare, Cleveland, OH, USA) with a 32-channel receiver head coil (Nova Medical, Wilmington, MA, USA) was used. The standard MRI protocol consisted of: a T1-weighted (3D acquisition; TI/TR/TE = 1225/4.8/2.2 ms; acquired voxel size = $1.00 \times 1.00 \times 1.00 \text{ mm}^3$; reconstructed = $0.66 \times 0.66 \times 0.50 \text{ mm}^3$), T2-weighted Turbo-Spin Echo (3D acquisition; TR/TE = 3158/301 ms; acquired voxel size = $0.70 \times 0.70 \times 0.70 \text{ mm}^3$; reconstructed = $0.35 \times 0.35 \times 0.35 \text{ mm}^3$), magnetization-prepared FLAIR (3D acquisition; TR/TE = 8000/300 ms; acquired voxel size = $0.80 \times 0.80 \times 0.80 \text{ mm}^3$; reconstructed = $0.49 \times 0.49 \times 0.49 \text{ mm}^3$), and a dual echo susceptibility-weighted imaging (SWI) (TR/TE1/TE2 = 20/6.9/15.8 ms; acquired voxel size = $0.50 \times 0.50 \times 0.70 \text{ mm}^3$; reconstructed = $0.40 \times 0.40 \times 0.35 \text{ mm}^3$) sequence.

Vessel wall MRI was performed with a T1-weighted Magnetization-Prepared Inversion Recovery Turbo Spin Echo sequence with the following settings: field of view $250 \times 250 \times 190 \text{ mm}^3$, acquired resolution $0.8 \times 0.8 \times 0.8 \text{ mm}^3$ (reconstructed to $0.49 \times 0.49 \times 0.4 \text{ mm}^3$), TR/TI/TE = 3952/1375/37 ms.²²

Assessment of ICAS

All patients were assessed by a trained observer (MHTZ) blinded to patient characteristics.¹⁶ MHTZ was trained by an experienced observer with eight years of experience with 7T vessel wall MRI 7T assessment (AGvdK). Of note, 7T vessel wall assessment was not blinded to the brain parenchyma, the latter of which is also visible on the vessel wall sequence, although with low tissue contrast. Therefore, assessments were performed zooming in on the vessel wall of interest. Lesions were rated according to recently published criteria.^{16,23} A lesion was defined as a diffuse or focal thickening of $\geq 50\%$ of the arterial wall, compared to the expected normal thickness, using the contralateral artery, or neighboring arterial segment as reference. Assessment was performed visually, and we did not measure lesion thickness. Lesions which were uncertain were assessed in multiple planes for verification. Lesions were rated per arterial segment, with each segment being able to contain multiple lesions, making the maximum lesion count theoretically unlimited. We rated the following segments: the anterior cerebral arteries (A1, A2 segments), middle cerebral arteries (M1, M2 segments), distal internal carotid arteries (ICA; supraclinoid (C6) and communicating segment (C7)), posterior communicating arteries, posterior cerebral arteries (P1, P2 segments, P1–P2 bifurcation), basilar artery, and vertebral arteries. A lesion which stretched into multiple segments was counted as a separate lesion for each segment. Lesions with eccentric and concentric components were regarded as separate lesions for each segment. An MR angiography sequence was not included in the 7T brain MRI protocol because of logistical reasons. As a result, we were not able to assess luminal stenosis.

Assessment of MRI markers of cerebrovascular disease

All assessments were performed by an experienced observer (MHTZ) blinded to patient characteristics. Assessment of 1.5T MRI was performed blinded to 7T MRI assessment and vice versa. Cortical infarcts, large subcortical infarcts, cerebellar infarcts, and lacunes of presumed vascular origin were visually rated on 1.5T MRI images, on the T1-weighted, T2-weighted, and FLAIR images. Cortical infarcts

were defined as a cortical or cortico-subcortical area of tissue necrosis with a minimum diameter of 4 mm to distinguish from cortical microinfarcts. Large subcortical infarcts were defined as a subcortical area of cavitated tissue necrosis >15 mm in minimum diameter to distinguish from lacunes. Cortical and subcortical infarcts were combined into “large subcortical and/or cortical infarcts” for further analyses, because both are thought to be primarily caused by large artery disease. Cerebellar cortical infarcts were defined as areas of tissue necrosis with involvement of the cerebellar cortex. Lacunes of presumed vascular origin were defined according to the STRIVE criteria.² In brief, a lacune was defined as a round or ovoid cerebrospinal fluid-filled subcortical lesion, 3–15 mm in size, with a variable FLAIR rim, and not being a perivascular space. A consensus was performed with an experienced neuroradiologist (TDW) for uncertain lesions. Cerebral cortical microinfarcts were rated on 7 T MRI, using the T1-weighted, T2-weighted, FLAIR, and SWI images, using standard rating criteria.²⁴ In short, a microinfarct was defined as a strictly intracortical lesion, visible in two or more directions, with a maximum diameter of 4 mm, which had to be hyperintense to cortex on T2-weighted imaging and hypointense on T1-weighted imaging, without an accompanying microbleed on SWI. Cerebral microbleeds were rated on the 7 T SWI source data and a reconstructed minimum intensity projection (slice thickness 4 mm, overlap 2 mm).²⁵ We distinguished lobar and deep microbleeds according to the Microbleed Anatomical Rating Scale.²⁶

White matter hyperintensity, gray matter, white matter, and CSF volumes were obtained with a previously validated probabilistic segmentation technique using *k*-nearest neighbor classification, on the 1.5 T T1-weighted, FLAIR, and T2-weighted inversion recovery sequences of the MR scans.²⁷ An investigator (RG) checked all white matter hyperintensity segmentations using an image processing framework (MeVisLab 2.7.1., MeVis Medical Solutions AG, Bremen, Germany) and manually adjusted incorrect segmentations. Infarcts were manually segmented (MHTZ) and subtracted from the other segmentation volumes in three-dimensional space. Volumes of gray matter, white matter, total white matter hyperintensity, and brain infarcts were summed to obtain total brain volume. Total intracranial volume was calculated by summing the total brain volume and the volume of the cerebrospinal fluid. Deep white matter hyperintensity was defined as >1 cm from the lateral ventricles, while periventricular white matter hyperintensity was defined as ≤1 cm of the lateral ventricles.

Statistical analysis

All analyses were performed using IBM SPSS Statistics version 25 for Windows (IBM Corporation, Armonk, NY, USA).

We performed multiple imputation with 10 datasets to address missing values. Analyses were performed by pooling the 10 imputed datasets.

ICAS burden, defined as the total number of vessel wall lesions per patient, was standardized into a Z-score and was used as the independent variable in all analyses. Modified Poisson regression with robust standard errors was used to calculate relative risks (RRs) for binary dependent variables. Standard linear regression was used to calculate unstandardized regression coefficients (*b*) for continuous dependent variables. Analyses were adjusted for age and sex in model 1, and additionally for educational level, BMI, smoking pack-years, alcohol use, diabetes, systolic and DBP, total cholesterol level, total high-density lipoprotein level, and use of antihypertensive, lipid-lowering, antiplatelet, or oral anticoagulant medication (model 2). In model 3, additional adjustments were made for carotid stenosis ≥50%, carotid intima-media thickness, and ankle-brachial index. All models of cerebral blood flow were additionally adjusted for total brain volume. All models of total brain volume and white matter hyperintensity volume were additionally adjusted for intracranial volume. White matter hyperintensity volumes were natural-log transformed before being entered into the model, to obtain a normal distribution. Residual plots of all linear regression analyses were checked for regression assumptions (e.g. normal distribution).

Finally, we stratified the study sample into a right-, left-dominant, or symmetric ICAS distribution and calculated descriptives of ICAS distribution and CSVD lesion distribution per hemisphere to explore co-localization between ICAS burden and CSVD. ICAS hemispheric dominance was defined as an interhemispheric difference of one or more vessel wall lesions. An interhemispheric difference of zero was defined as symmetric.

Data availability statement

For use of anonymized data, a reasonable request has to be made in writing to the study group, and the third party has to sign a confidentiality agreement.

Results

Table 1 shows the characteristics of the study sample (*N* = 130; 88% male; 68 ± 9 years). Table 2 gives an overview of the MRI neuroimaging markers in the study sample. Brain infarcts were commonly found,

Table 1. Characteristics of study sample ($N = 130$).

Age (years)	68 ± 9
Men (%)	88%
Body mass index (kg/m^2)	27.3 ± 3.7
Educational level (range 1–7) ^a	5 (2, 6)
Smoking pack-years ^a	19.8 (0.0, 43.4)
Alcohol use (%)	
1–10 units/week	43%
>11 units/week	29%
Systolic blood pressure (mmHg)	139 ± 17
Diastolic blood pressure (mmHg)	79 ± 9
Cholesterol, mmol/L	
LDL-C	2.4 ± 0.8
HDL-C	1.3 ± 0.4
Total	4.4 ± 0.9
Diabetes (%)	19%
Carotid stenosis ≥50%	10%
Carotid intima-media thickness (mm)	0.85 ± 0.23
Ankle–brachial index	1.09 ± 0.18
History of vascular disease (%) ^b	
Coronary heart disease	82%
Cerebrovascular disease	19%
Peripheral arterial disease	19%
Abdominal aortic aneurysm	2%
Medication use (%)	
Antihypertensive medication	83%
Lipid-lowering medication	90%
Antiplatelet medication	89%
Oral anticoagulants	10%

Note: Values are presented as mean ± SD or frequencies (as %).

^aMedian (10th, 90th percentile).

^bComorbid disease is possible.

Table 2. MRI markers of cerebrovascular disease in study sample ($N = 130$).

Brain infarcts	
Cortical infarcts	6.2%
Large subcortical infarcts	3.1%
Lacunes of presumed vascular origin	16.2%
Cerebellar infarcts	11.5%
Cortical microinfarcts	13.1%
Microbleeds	
Any microbleeds	57%
Lobar microbleeds	53%
Deep microbleeds	32%
Brain volumes	
Brain volume (ml)	1128 ± 98
Total WMH volume (ml) ^a	1.5 (0.3, 9.04)
Periventricular WMH volume (ml) ^a	1.2 (0.2, 8.5)
Deep WMH volume (ml) ^a	0.2 (0.0, 1.0)
Cerebral blood flow (ml/min)	526 ± 105

Note: Values are presented as mean ± SD or frequencies (%).

^aMedian (10th, 90th percentile).

WMH: white matter hyperintensities.

lacunes of presumed vascular origin being most common with a frequency of 16%. In addition, there was a high prevalence of microbleeds, with 57% of participants having ≥1 microscopic hemorrhage. Vessel wall lesions were found in 96% of patients, with a mean ICAS burden of 8.5 ± 5.7 lesions (median 7, range 0–32). A mean ICAS burden of 5.3 ± 3.2 lesions (median 4, range 0–14) was found in the anterior circulation, and a mean ICAS burden of 3.8 ± 3.0 lesions (median 3; range 0–18) was found in the posterior circulation. A detailed overview of the vessel wall lesion distribution can be found in our prior publication.¹⁶ Figure 1 presents an example of vessel wall lesions on 7T vessel wall MRI and the parenchymal lesions associated with a higher number of vessel wall lesions (i.e. higher ICAS burden).

Table 3 presents the RR of brain infarcts per +1 SD in ICAS burden, calculated using modified Poisson regression analysis. ICAS burden was associated with presence of large subcortical and/or cortical infarcts (RR = 1.65; 95% CI: 1.12–2.43), lacunes of presumed vascular origin (RR = 1.45; 95% CI: 1.14–1.86), and cortical microinfarcts (RR = 1.48; 95% CI: 1.13–1.94), after adjustment for age, sex, vascular risk factors, and medication use. Additional adjustment for carotid stenosis ≥50%, carotid intima-media thickness, and ankle–brachial index caused no considerable change. No significant association was found with cerebellar infarcts (RR = 1.15; 95% CI: 0.78–1.70), after adjustment for age, sex, vascular risk factors, and medication use.

Table 4 presents the RR of microbleeds per +1 SD in ICAS burden, calculated using modified Poisson regression analysis. As can be seen, no association was found with presence of microbleeds at any, lobar, or deep location.

Table 5 presents the unstandardized regression coefficient estimates for total brain volume, white matter hyperintensity volumes, and cerebral blood flow, per +1 SD in ICAS burden. ICAS burden was associated with natural-log transformed total white matter hyperintensity volume ($b = 0.24$; 95% CI: 0.02–0.46) and natural-log transformed periventricular white matter hyperintensity volume ($b = 0.32$; 95% CI: 0.08–0.56), but not deep white matter hyperintensity volume, after adjustment for age, sex, intracranial volume, vascular risk factors, and medication use. Additional adjustment for carotid stenosis ≥50%, carotid intima-media thickness, and ankle–brachial index caused no considerable change. A non-significant association between higher ICAS burden and lower cerebral blood flow was found ($b = -15.24$ ml/min; 95% CI: -34.85 to 4.38). Note, analyses of cerebral blood flow were additionally adjusted for total brain volume in all models. No

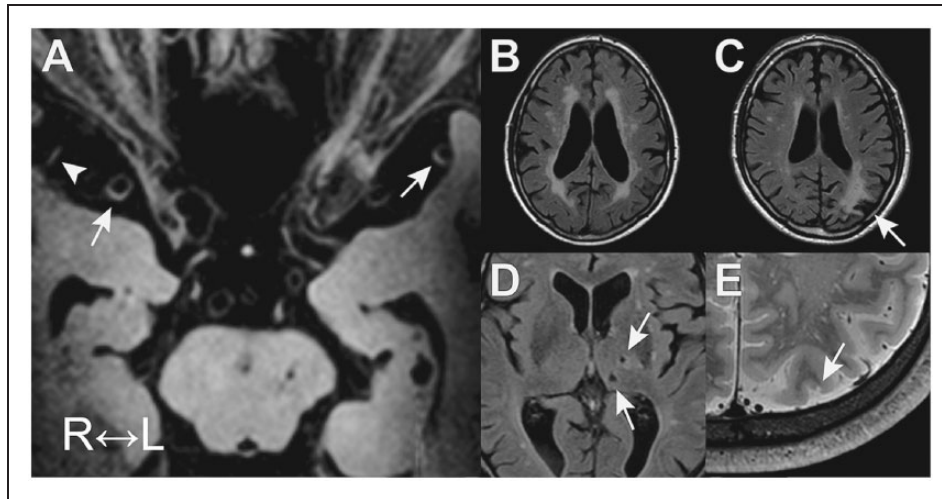


Figure 1. Examples of intracranial vessel wall lesions on 7T vessel wall MRI (a) and associated parenchymal lesions (b) to (e). (a): Vessel wall lesions in the M1 segment on both sides (arrows) and M2 lesion on the right (arrowhead); (b): periventricular white matter hyperintensities; (c): cortical infarct (arrow); (d): lacunes of presumed vascular origin (arrows); and (e): cortical microinfarct (arrow).

Table 3. Association between ICAS burden and presence of brain infarcts (yes vs. no).

Model	Large subcortical/ cortical infarcts ^b RR (95% CI)	Lacunes RR (95% CI)	Cerebellar infarcts RR (95% CI)	Cortical microinfarcts RR (95% CI)
ICAS burden ^a				
1	1.71 (1.34–2.19)	1.50 (1.19–1.89)	1.28 (0.87–1.86)	1.62 (1.29–2.03)
2	1.65 (1.12–2.43)	1.45 (1.14–1.86)	1.15 (0.78–1.70)	1.48 (1.13–1.94)
3	1.56 (1.12–2.27)	1.41 (1.10–1.82)	1.10 (0.72–1.70)	1.43 (1.07–1.94)

Notes: Values are relative risks (RR) with 95% confidence intervals calculated with modified Poisson regression analysis with robust error variance. Model 1: adjusted for age and sex. Model 2: model 1 + adjustment for educational level, body mass index, smoking pack-years, alcohol use, diabetes, systolic/diastolic blood pressure, total cholesterol level, total high-density lipoprotein level, and use of antihypertensive, lipid-lowering, antiplatelet, or oral anticoagulant medication. Model 3: model 2 + adjustment for carotid stenosis $\geq 50\%$, carotid intima-media thickness, or ankle-brachial index.

^aStandardized into Z-score.

^bDefined as presence of large subcortical infarcts and/or cortical infarcts.

Table 4. Association between ICAS burden and presence of cerebral microbleeds (yes vs. no).

Model	Any microbleed RR (95% CI)	Lobar microbleeds RR (95% CI)	Deep microbleeds RR (95% CI)
ICAS burden ^a			
1	1.04 (0.89–1.21)	1.03 (0.86–1.23)	1.14 (0.91–1.42)
2	1.09 (0.92–1.29)	1.10 (0.90–1.34)	1.18 (0.92–1.51)
3	1.10 (0.93–1.30)	1.11 (0.91–1.35)	1.19 (0.92–1.54)

Notes: Values are relative risks (RR) with 95% confidence intervals calculated with modified Poisson regression analysis with robust error variance. Model 1: adjusted for age and sex. Model 2: model 1 + adjustment for educational level, body mass index, smoking pack-years, alcohol use, diabetes, systolic/diastolic blood pressure, total cholesterol level, total high-density lipoprotein level, and use of antihypertensive, lipid-lowering, antiplatelet, or oral anticoagulant medication. Model 3: model 2 + adjustment for carotid stenosis $\geq 50\%$, carotid intima-media thickness, or ankle-brachial index.

^aStandardized into Z-score.

association was found between ICAS burden and total brain volume.

Table 6 shows the descriptives of the ICAS and CSVD lesion distribution between the right and left hemispheres stratified by ICAS distribution dominance. As expected, the mean number of vessel wall

lesions was similar in the symmetric group, higher in the left circulation in the left-dominant group, and higher in the right circulation in the right-dominant group. In the group with a right hemispheric dominance of vessel wall lesions, the white matter hyperintensity volume was quite symmetric. If anything,

Table 5. Association between ICAS burden and brain volumes and cerebral blood flow.

Model	ICAS burden ^a	Total brain volume (ml)	Total WMH volume (ml) ^b	Periventricular WMH volume (ml) ^b	Deep WMH volume (ml) ^b	Cerebral blood flow (ml/min) ^c
		<i>b</i> (95% CI)	<i>b</i> (95% CI)	<i>b</i> (95% CI)	<i>b</i> (95% CI)	<i>b</i> (95% CI)
1	1	0.34 (−5.05 to 5.73)	0.24 (0.04 to 0.43)	0.31 (0.1 to 0.52)	0.02 (−0.21 to 0.25)	−15.62 (−32.97 to 1.72)
2	2	1.99 (−4.01 to 7.98)	0.24 (0.02 to 0.46)	0.32 (0.08 to 0.56)	0.01 (−0.26 to 0.26)	−15.24 (−34.85 to 4.38)
3	3	2.14 (−3.92 to 8.2)	0.25 (0.03 to 0.48)	0.33 (0.10 to 0.57)	0.01 (−0.26 to 0.27)	−12.39 (−31.87 to 7.09)

Values are unstandardized linear regression coefficients (*b*) with 95% confidence intervals calculated with standard linear regression analysis.

Model 1: adjusted for age and sex. Model 2: model 1 + adjustment for educational level, body mass index, smoking pack-years, alcohol use, diabetes, systolic/diastolic blood pressure, total cholesterol level, total high-density lipoprotein level, use of antihypertensive, lipid-lowering, antiplatelet or oral anticoagulant medication. Model 3: model 2 + adjustment for carotid stenosis $\geq 50\%$, carotid intima-media thickness or ankle-brachial index.

^aStandardized into Z-score.

^bNatural-log transformed.

^cAnalyses of cerebral blood flow were additionally adjusted for total brain volume in all models.

WMH: white matter hyperintensities.

Table 6. Descriptives of CSVD lesion distribution stratified by left vs. right dominant or symmetric ICAS distribution.

ICAS dominance	ICAS burden (no. lesions)		WMH volume (% ICV) ^a		Lacunes present (%)		CMLs present (%)	
	Right	Left	Right	Left	Right	Left	Right	Left
	Symmetric (<i>n</i> = 29)	4.1	4.1	0.10 (0.02, 0.68)	0.10 (0.03, 0.64)	10%	3%	10%
Right (<i>n</i> = 45)	5.1	3.6	0.11 (0.02, 0.49)	0.09 (0.01, 0.56)	9%	16%	7%	13%
Left (<i>n</i> = 56)	3.0	4.8	0.10 (0.02, 0.56)	0.09 (0.02, 0.57)	11%	11%	9%	5%

Note: right indicates right hemisphere and left indicates left hemisphere.

^aMedian (10th, 90th percentile).

WMH: white matter hyperintensities; ICV: intracranial volume; CMLs: cortical microinfarcts.

lacunes and microinfarcts were more present in the left hemisphere. In the group with a left hemispheric dominance of vessel wall lesions, white matter hyperintensity volume and lacune presence was quite symmetric and lacunes were more present on the right.

Discussion

In this cohort of 130 patients with a history of vascular disease, vessel wall lesions on 7 T MRI were very common and a higher number of lesions was associated with large subcortical and/or cortical infarcts as well as MRI features of CSVD, including lacunes of presumed vascular origin, periventricular and total white matter hyperintensity volume, and cortical microinfarcts.

Our findings regarding lacunes are in concordance with early post-mortem studies^{7,28} and a few neuroimaging studies in Asian populations,^{8,9} but contradict the conclusion of a study in whites with lacunar stroke.⁵ A possible explanation for the latter discrepancy could be the difference in ICAS imaging: ultra-high field vessel wall MRI versus transcranial Doppler ultrasound. Furthermore, we found an association between vessel wall lesions and white matter

hyperintensities. Although a relation between ICAS and white matter lesions is a matter of ongoing dispute,²⁹ several studies have found associations with ICAS,^{30–32} and with carotid stenosis.^{33–35} Our findings add to the growing body of evidence that ICAS is related to white matter hyperintensities. Moreover, we found an association between vessel wall lesions and cortical microinfarcts, which is in line with the few small in vivo studies published on this subject.^{36–38} A possible pathway linking vessel wall lesions to these CSVD features could be steno-occlusive disease or (micro)embolisms; both can lead to downstream ischemic lesions.²⁴

We did not find an association between vessel wall lesions and microbleeds. However, this seems in concordance with the view that incidental microbleeds are generally caused by intrinsic small vessel disease, e.g. hypertensive vasculopathy and cerebral amyloid angiopathy.³⁹ Although we observed an association between higher numbers of vessel wall lesions and lower cerebral blood flow, it did not reach statistical significance. Vessel wall thickening can cause a reduction of downstream cerebral blood flow by means of luminal stenosis.⁴⁰ Unfortunately, we do not have data

on stenosis grade, because we did not include an MR angiography sequence in our protocol. A possible explanation for the absent association is that the effect of the hemodynamically-significant stenotic lesions is attenuated by a bulk of non-stenotic lesions. However, we have no way to examine this. Finally, no association was found between ICAS and total brain volume. As far as we know, no prior studies have observed this association, although associations between carotid stenosis and cerebral atrophy have been observed.^{34,41}

Our study has several strengths. First, 7 T vessel wall MRI enabled visualization of the actual pathology, which is located in the vessel wall, enabling identification of ICAS independent of luminal stenosis. In addition, the large coverage area and increased contrast-to-noise ratio compared to lower field strengths facilitated a more complete and accurate assessment of ICAS than is possible at lower field strengths. Furthermore, we were able to examine various MRI markers of large vessel and small vessel disease within one study and data on vascular risk factors and medication use allowed to adjust for possible confounding factors. Finally, microinfarcts and microbleeds were assessed on 7 T field strength, which is the most sensitive field strength for these lesions *in vivo*.

Several limitations also need to be addressed. First, because the data were analyzed cross-sectionally, we cannot draw any conclusions regarding causality. Second, there is a lack of radiopathologic correlation studies on intracranial vessel wall lesions, which leaves the possibility that not all lesions are of atherosclerotic pathology. However, this is a limitation of all current vessel wall imaging studies. Furthermore, we think the *a priori* probability of a lesion being non-atherosclerotic (e.g. dissection, vasculitis), especially in our population and study setting, is very low. Additionally, their correlation with vascular risk factors¹⁶ and extracranial atherosclerosis,¹⁷ further supports its use as a marker of ICAS. Third, our study sample has a high burden of manifest arterial disease and high frequency of vascular risk factors, which may have limited power to adjust for these factors. We tried to carefully adjust for these vascular risk factors by adding continuous (e.g. pack-years of smoking, blood pressure) instead of dichotomous measures (e.g. smoking, hypertension) to the models, which resulted in higher variability in risk factor exposure. Studies in different settings are needed to see if the observed relationships can be generalized to the other populations. Fourth, although vessel assessment was blinded to 1.5 T and 7 T brain MRI assessment, it was not blinded to the brain parenchyma, the latter of which is also visible on the vessel wall sequence. However, the intraparenchymal contrast is very low and assessment was

performed zoomed in on the vessel of interest. Nonetheless, a large cortical infarct is difficult to overlook and could have involuntarily lead to more thorough assessment of the vessel walls. Of note, white matter hyperintensities and microinfarcts are not easily visible on this sequence, and were also associated with ICAS. Finally, a large majority of our study sample were taking one or more vascular medications, which might have modified the association between ICAS and MRI features of CSVD. Due to the sample size, we were not able to stratify analyses on medication use.

Our findings have importance because the association between vessel wall lesions and MRI features of CSVD suggests that ICAS might have a role in the etiology of MRI features CSVD. However, ICAS burden could also be a marker of intracranial large and small vessel disease. Meaning, the severity of large and small vessel disease is correlated, e.g. due to shared risk, but it is the small artery disease that causes the brain lesions. As we did not image the actual small vessels—but only the parenchymal sequelae on MRI, we cannot reliably untangle this. Furthermore, we did not find evidence of co-location of ICAS and CSVD lesions, which could have strengthened the case for causality. Future studies should try to functionally and structurally visualize the small(est) vessels and large vessels and test if they are differentially associated with MRI markers of CSVD, preferably in a longitudinal study design. Apart from this, the co-occurrence could still help explain part of the heterogeneity of CSVD¹⁰ (e.g. in regard to clinical functioning).

In conclusion, a higher ICAS burden was associated with more MRI features of CSVD, although no evidence of co-location was observed. Further longitudinal studies, preferably employing high-resolution vascular imaging,^{42,43} are required to determine if ICAS precedes development of CSVD.

Funding

The author(s) disclosed receipt of the following financial support for the research, authorship, and/or publication of this article: The research of Jeroen Hendrikse has received funding from the European Research Council under the European Union's Horizon 2020 Programme (H2020)/ERC grant agreement no. 637024 (HEARTOFSTROKE) and H2020 grant agreement no. 666881, SVDs@target. Jeroen Hendrikse is supported by the Netherlands Organization for Scientific Research (NWO) under grant no. 91712322.

Acknowledgements

We gratefully acknowledge the contribution of the SMART research nurses; R van Petersen (data-manager); BGF Dinther (vascular manager), and the members of the

Utrecht Cardiovascular Cohort-Second Manifestations of ARterial disease-Studygroup (UCC-SMART-Studygroup): FW Asselbergs and HM Nathoe, Department of Cardiology; GJ de Borst, Department of Vascular Surgery; ML Bots and MI Geerlings, Julius Center for Health Sciences and Primary Care; MH Emmelot, Department of Geriatrics; PA de Jong and T Leiner, Department of Radiology; AT Lely, Department of Obstetrics & Gynecology; NP van der Kaaij, Department of Cardiothoracic Surgery; LJ Kappelle and YM Ruijgrok, Department of Neurology; MC Verhaar, Department of Nephrology; and FLJ Visseren (chair) and J Westerink, Department of Vascular Medicine, University Medical Center Utrecht and Utrecht University.

Declaration of conflicting interests

The author(s) declared no potential conflicts of interest with respect to the research, authorship, and/or publication of this article.


Authors' contributions

Maarten HT Zwartbol: MRI image analysis, literature search, figures, data collection, data analysis, data interpretation, and writing. Anja G van der Kolk: MRI image analysis, data interpretation, and critically reviewed the manuscript. Hugo J Kuijf: MRI image analysis and critically reviewed the manuscript. Theo D Witkamp: MRI image analysis and critically reviewed the manuscript. Rashid Ghaznawi: MRI image analysis, data collection, and critically reviewed the manuscript. Jeroen Hendrikse: study design and critically reviewed the manuscript. Mirjam I Geerlings: study design, data interpretation, data analysis, and critically reviewed the manuscript.

ORCID iDs

Maarten HT Zwartbol  <https://orcid.org/0000-0001-5779-3150>

Hugo J Kuijf  <https://orcid.org/0000-0001-6997-9059>

Rashid Ghaznawi  <https://orcid.org/0000-0002-6616-5276>

References

- Pantoni L. Cerebral small vessel disease: from pathogenesis and clinical characteristics to therapeutic challenges. *Lancet Neurol* 2010; 9: 689–701.
- Wardlaw JM, Smith EE, Biessels GJ, et al.; STandards for ReportIng Vascular Changes on nEuroimaging (STRIVE v1). Neuroimaging standards for research into small vessel disease and its contribution to ageing and neurodegeneration. *Lancet Neurol* 2013; 12: 822–838.
- Wardlaw JM, Smith C and Dichgans M. Mechanisms of sporadic cerebral small vessel disease: insights from neuroimaging. *Lancet Neurol* 2013; 12: 532.
- Wardlaw JM, Smith C and Dichgans M. Small vessel disease: mechanisms and clinical implications. *Lancet Neurol* 2019; 18: 684–696.
- Wardlaw JM, Doubal FN, Eadie E, et al. Little association between intracranial arterial stenosis and lacunar stroke. *Cerebrovasc Dis* 2011; 31: 12–18.
- Arenillas JF, Lopez-Cancio E and Wong KS. Biomarkers, natural course and prognosis. *Front Neurol Neurosci* 2016; 40: 93–108.
- Fisher C. Lacunar infarcts – a review. *Cerebrovasc Dis* 1991; 1: 311–320.
- Chung J-W, Kim BJ, Sohn CH, et al. Branch atheromatous plaque: a major cause of lacunar infarction (high-resolution MRI study). *Cerebrovasc Dis Extra* 2012; 2: 36–44.
- Miyaji Y, Kawabata Y, Joki H, et al. High-resolution magnetic resonance imaging findings of basilar artery plaque in a patient with branch atheromatous disease: a case report. *J Med Case Rep* 2014; 8: 1–3.
- Ter Telgte A, Van Leijssen EMC, Wiegertjes K, et al. Cerebral small vessel disease: from a focal to a global perspective. *Nat Rev Neurol* 2018; 14: 387–398.
- Degnan AJ. Underestimating the importance of Middle cerebral artery atherosclerosis in lacunar stroke. *Cerebrovasc Dis* 2011; 32: 301.
- Mandell DM, Mossa-Basha M, Qiao Y, et al.; Vessel Wall Imaging Study Group of the American Society of Neuroradiology. Intracranial vessel wall MRI: principles and expert consensus recommendations of the American society of neuroradiology. *AJNR Am J Neuroradiol* 2017; 38: 218–229.
- Qiao Y, Anwar Z, Intrapromkul J, et al. Patterns and implications of intracranial arterial remodeling in stroke patients. *Stroke* 2016; 47: 434–440.
- Zhu C, Haraldsson H, Tian B, et al. High resolution imaging of the intracranial vessel wall at 3 and 7 T using 3D fast spin echo MRI. *MAGMA* 2016; 29: 559–570.
- Hartevelde AA, Van der Kolk AG, Van der Worp HB, et al. High-resolution intracranial vessel wall MRI in an elderly asymptomatic population: comparison of 3T and 7T. *Eur Radiol* 2017; 27: 1585–1595.
- Zwartbol MHT, Van der Kolk AG, Ghaznawi R, et al.; SMART Study Group. Intracranial vessel wall lesions on 7T MRI (magnetic resonance imaging). *Stroke* 2019; 50: 88–94.
- Zwartbol MHT, Geerlings MI, Ghaznawi R, et al.; UCC-SMART Study Group. Intracranial atherosclerotic burden on 7T MRI is associated with markers of extracranial atherosclerosis: the SMART-MR study. *AJNR Am J Neuroradiol* 2019; 40: 2016–2022.
- Geerlings MI, Appelman AP, Vincken KL, et al.; SMART Study Group. Brain volumes and cerebrovascular lesions on MRI in patients with atherosclerotic disease. The SMART-MR study. *Atherosclerosis* 2010; 210: 130–136.
- Appelman APA, Van Der Graaf Y, Vincken KL, et al.; SMART Study Group. Total cerebral blood flow, white matter lesions and brain atrophy: the SMART-MR study. *J Cereb Blood Flow Metab* 2008; 28: 633–639.
- Knoops AJ, Gerritsen L, Van der Graaf Y, et al. Basal hypothalamic pituitary adrenal axis activity and hippocampal volumes: the SMART-Medea study. *Biol Psychiatry* 2010; 67: 1191–1198.

21. Simons PCG, Algra A, Van De Laak MF, et al. Second manifestations of ARterial disease (SMART) study: rationale and design. *Eur J Epidemiol* 1999; 15: 773–781.
22. Van der Kolk AG, Hendrikse J, Brundel M, et al. Multi-sequence whole-brain intracranial vessel wall imaging at 7.0 tesla. *Eur Radiol* 2013; 23: 2996–3004.
23. Lindenholz A, Van der Kolk AG, Zwanenburg JJM, et al. The use and pitfalls of intracranial vessel wall imaging: how we do it. *Radiology* 2018; 286: 12–28.
24. Van Veluw SJ, Shih AY, Smith EE, et al. Detection, risk factors, and functional consequences of cerebral microinfarcts. *Lancet Neurol* 2017; 16: 730–740.
25. De Bresser J, Brundel M, Conijn MM, et al. Visual cerebral microbleed detection on 7T MR imaging: reliability and effects of image processing. *Am J Neuroradiol* 2013; 34: E61–E64.
26. Gregoire SM, Chaudhary UJ, Brown MM, et al. The microbleed anatomical rating scale (MARS): reliability of a tool to map brain microbleeds. *Neurology* 2009; 73: 1759–1766.
27. Anbeek P, Vincken KL, Van Osch MJ, et al. Probabilistic segmentation of white matter lesions in MR imaging. *Neuroimage* 2004; 21: 1037–1044.
28. Fisher CM. The arterial lesions underlying lacunes. *Acta Neuropathol* 1968; 12: 1–15.
29. Topakian R. Conflicting evidence on the association of white matter hyperintensities with large-artery disease. *Eur J Neurol* 2015; 22: 4–5.
30. Nam K-WW, Kwon H-MM, Jeong H-YY, et al. Cerebral white matter hyperintensity is associated with intracranial atherosclerosis in a healthy population. *Atherosclerosis* 2017; 265: 179–183.
31. Park J-HH, Kwon H-MM, Lee J, et al. Association of intracranial atherosclerotic stenosis with severity of white matter hyperintensities. *Eur J Neurol* 2015; 22: 44–52.
32. Lee SJ, Kim JS, Chung SW, et al. White matter hyperintensities (WMH) are associated with intracranial atherosclerosis rather than extracranial atherosclerosis. *Arch Gerontol Geriatr* 2011; 53: e129–e132.
33. Romero JR, Beiser A, Seshadri S, et al. Carotid artery atherosclerosis, MRI indices of brain ischemia, aging, and cognitive impairment: the Framingham study. *Stroke* 2009; 40: 1590–1596.
34. Manolio TA, Burke GL, O’Leary DH, et al. Relationships of cerebral MRI findings to ultrasonographic carotid atherosclerosis in older adults: the cardiovascular health study. *Arterioscler Thromb Vasc Biol* 1999; 19: 356–365.
35. Bos D, Ikram MA, Elias-Smale SE, et al. Calcification in major vessel beds relates to vascular brain disease. *Arterioscler Thromb Vasc Biol* 2011; 31: 2331–2337.
36. Hilal S, Sikking E, Shaik MA, et al. Cortical cerebral microinfarcts on 3T MRI: a novel marker of cerebrovascular disease. *Neurology* 2016; 87: 1583–1590.
37. Dieleman N, Van der Kolk AG, Zwanenburg JJ, et al. Relations between location and type of intracranial atherosclerosis and parenchymal damage. *J Cereb Blood Flow Metab* 2016; 36: 1271–1280.
38. Van Veluw SJ, Hilal S, Kuijf HJ, et al. Cortical microinfarcts on 3T MRI: clinical correlates in memory-clinic patients. *Alzheimers Dement* 2015; 11: 1500–1509.
39. Greenberg SM, Vernooij MW, Cordonnier C, et al.; Microbleed Study Group. Cerebral microbleeds: a field guide to their detection and interpretation. *Lancet Neurol* 2009; 8: 165–174.
40. Pu Y, Lan L, Leng X, et al. Intracranial atherosclerosis: from anatomy to pathophysiology. *Int J Stroke* 2017; 12: 236–245.
41. Muller M, Van der Graaf Y, Algra A, et al.; SMART Study Group. Carotid atherosclerosis and progression of brain atrophy: the SMART-MR study. *Ann Neurol* 2011; 70: 237–244.
42. De Cockler LJ, Lindenholz A, Zwanenburg JJ, et al. Clinical vascular imaging in the brain at 7 T. *Neuroimage* 2018; 168: 452–458.
43. Geurts LJ, Zwanenburg JJM, Klijn CJM, et al. Higher pulsatility in cerebral perforating arteries in patients with small vessel disease related stroke, a 7T MRI study. *Stroke* 2019; 50: 62–68.